

ANALYSIS OF THE SPHERICAL WAVE TRUNCATION ERROR FOR SPHERICAL HARMONIC SOUNDFIELD EXPANSIONS

Stefanie Brown^{*}, Shuai Wang^{*} and Deep Sen^{*†}

^{*}Acoustics Laboratory, School of Electrical Engineering and Telecommunications
The University of New South Wales, Sydney, Australia
Email: {stefanie, s.wang, d.sen}@unsw.edu.au

[†]Qualcomm Inc., Audio Research & Development, San Diego, CA, USA

ABSTRACT

Three dimensional soundfield recording and reproduction is an area of ongoing investigation and its implementation is increasingly achieved through use of the infinite Spherical Harmonic soundfield expansion. Perfect recording or reconstruction requires infinite microphones or loudspeakers, respectively. Thus, real-world approximations to both require spatial discretisation, which truncates the soundfield expansion and loses some of the soundfield information. The resulting truncation error is the focus of this paper, specifically for soundfields comprising of spherical waves. We define two norms of the truncation error to signal ratio, L_2 and L_∞ , for comparison and use in different situations. Finally we observe how some of these errors converge to the plane wave case under certain circumstances.

Index Terms— Acoustic signal processing, spherical harmonic expansion, truncation error, spherical waves

1. INTRODUCTION

Multichannel recording and reproduction of three dimensional soundfields has attracted much attention from researchers in recent times, especially using the Spherical Harmonic expansion because of its spatial representation of the soundfield. Applications include beamforming and immersive soundfield reproduction amongst others. Both recording and reproduction processes are complicated by the introduction of errors due to several factors, some of which have been investigated in the literature e.g. small positional errors of microphones [1] and/or loudspeakers, the method used to convert microphone signals into spherical harmonic coefficients and back into speaker feeds [2] and lastly the truncation error inherent in using spatially discrete media to record/reproduce the sound field [3, 4].

Estimating the truncation error is very important as it is impossible to eliminate. Definitions vary between authors e.g. the unnormalised upper bound of the truncation error on the sphere [4] or the normalised truncation error to signal ratio, integrated over the sphere [3]. However, these papers have investigated truncation errors in the context of the farfield, i.e. plane wave soundfields only, and the analysis in [3] places restrictions on the maximum frequency and radius of the low error region. The use of different metrics of the truncation error makes comparison between them difficult. In this paper, we examine the truncation error for near-field spherical waves and propose two truncation error to signal ratio metrics based on the L_2 and L_∞ norms that can be used given certain restrictions on the soundfield.

This paper firstly introduces the conventions and definitions for functions used throughout. It then discusses the two types of truncation error and derives results for them for spherical waves. Finally it observes if and how these error definitions converge to previously derived plane wave solutions.

2. BACKGROUND

We have found that conventions and notations used in this field vary widely between and even amongst research groups. As such, we find it prudent to specify the assumptions we have made to avoid confusion.

2.1. Conventions

Spherical coordinates are defined by $\mathbf{r} = (r, \theta, \phi)$ as the radius, angle of inclination from the positive z-axis and angle of azimuth from the positive x-axis respectively.

The engineering convention for the DFT is used. As such, unit amplitude plane waves are defined as (1) and spherical waves are defined as (2). ω and k are the angular frequency and wave number, $\mathbf{k} = -k\hat{\mathbf{x}}_s$ and $\mathbf{r}_s = (r_s, \theta_s, \phi_s)$ is the source location.

$$p(t, \mathbf{r})_{\text{pl}} = \exp\{i(\omega t - \mathbf{k} \cdot \mathbf{r})\} \quad (1)$$

$$p(t, \mathbf{r})_{\text{sph}} = \frac{\exp\{i(\omega t - k|\mathbf{r} - \mathbf{r}_s|)\}}{|\mathbf{r} - \mathbf{r}_s|} \quad (2)$$

2.2. Definitions

The definition of the spherical harmonic of mode (n, m) used is:

$$Y_n^m(\theta, \phi) = \sqrt{\frac{2n+1}{4\pi} \frac{(n-|m|)!}{(n+|m|)!}} P_n^{|m|}(\cos(\theta)) e^{im\phi} \quad (3)$$

The general solution to the wave equation in a non-scattering environment is:

$$p(t, k, \mathbf{r}) = P(k, \mathbf{r}) \times e^{i\omega t} \\ = \left[\sum_{n=0}^{\infty} j_n(kr) \sum_{m=-n}^n A_n^m(k) Y_n^m(\theta, \phi) \right] e^{i\omega t} \quad (4)$$

$P(k, \mathbf{r})$ can be separated into two components: the truncated signal comprising of terms from orders 0 to N and the truncation remainder comprising of terms of order $n > N$. The various error

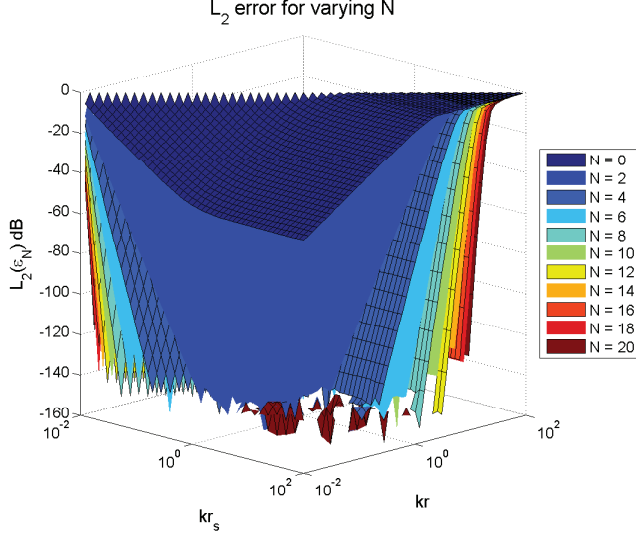


Fig. 1. L_2 error (dB) with N varying from 0 to 20.

types described herein are permutations of this remainder. $j_n(kr)$ is the spherical Bessel function.

$$\text{Remainder} = \sum_{n>N} j_n(kr) \sum_{m=-n}^n A_n^m(k) Y_n^m(\theta, \phi) \quad (5)$$

The spherical harmonic coefficients A_n^m are defined for plane waves and the interior solution of for spherical waves below. They are modified from [5] such that both plane and spherical waves use the engineering Fourier transform convention and that (θ_s, ϕ_s) is the direction of the spherical wave source, but is anti-parallel to the direction of equivalent plane wave. The interior solution holds true for $r < r_s$ [6].

$$A_{n\text{ pl}}^m(k) = 4\pi i^n Y_n^{m*}(\theta_s, \phi_s) \quad (6)$$

$$A_{n\text{ sph}}^m(k) = -4\pi i k h_n^{(2)}(kr_s) Y_n^{m*}(\theta_s, \phi_s) \quad (7)$$

where $h_n^{(2)}(kr_s)$ is the spherical Hankel function of the second kind.

We will define the L_q error to signal ratio as

$$L_q(\epsilon_N) = \left(\frac{\int |P - P_N|^q d\Omega}{\int |P|^q d\Omega} \right)^{1/q} = \left(\frac{f_q}{g_q} \right)^{1/q} \quad (8)$$

where P refers to the pressure signal $P(k, \mathbf{r})$, P_N refers to the truncated signal up to order N and $\int d\Omega$ is the integral over the unit sphere. We have defined f_q and g_q as the numerator and denominator of the error function inside the q^{th} root, as they will be calculated separately for convenience in the analysis.

3. L_2 ERROR

The L_2 error represents an averaging of the truncation error over the sphere. We define it to be

$$L_2(\epsilon_N) = \left(\frac{\int |P - P_N|^2 d\Omega}{\int |P|^2 d\Omega} \right)^{1/2} \quad (9)$$

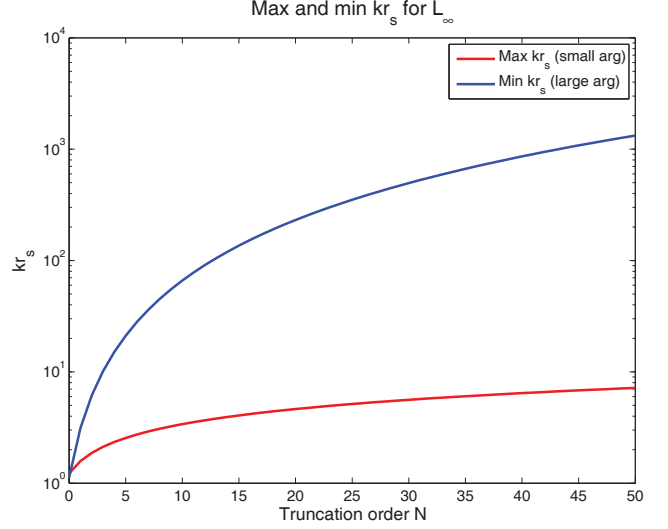


Fig. 2. Restrictions on the values of kr_s for various orders N .

The numerator of this may be calculated for spherical waves following the method in [3], making use of the orthonormality and addition theorems for spherical harmonics [6].

$$f_2 = \int |P - P_N|^2 d\Omega = \int \left| \sum_{n>N} j_n(kr) \sum_{m=-n}^n A_n^m(k) Y_n^m(\theta, \phi) \right|^2 d\Omega \quad (10)$$

$$= \sum_{n>N} \sum_{m=-n}^n \sum_{p>N} \sum_{q=-p}^p j_n(kr) j_p(kr) \times A_n^m A_p^{q*} \times \int Y_n^m(\theta, \phi) Y_p^{q*}(\theta, \phi) d\Omega = \sum_{n>N} (4\pi k)^2 j_n(kr)^2 |h_n(kr_s)|^2 \frac{2n+1}{4\pi} P_n(\hat{\mathbf{r}}_s \cdot \hat{\mathbf{r}}_s) \quad (11)$$

$$= 4\pi k^2 \sum_{n>N} (2n+1) j_n(kr)^2 (j_n(kr_s)^2 + y_n(kr_s)^2) \quad (12)$$

Similarly, the pressure function g_2 can be expressed as

$$g_2 = 4\pi k^2 \sum_{n=0}^{\infty} (2n+1) j_n(kr)^2 (j_n(kr_s)^2 + y_n(kr_s)^2) \quad (13)$$

As such f_2 can be re-written as (14) and g_2 as (15), which is independent of the source direction.

$$f_2 = g_2 - 4\pi k^2 \sum_{n=0}^N (2n+1) j_n(kr)^2 (j_n(kr_s)^2 + y_n(kr_s)^2) \quad (14)$$

$$g_2 = \int \left| \frac{e^{-ik|\mathbf{r}-\mathbf{r}_s|}}{|\mathbf{r}-\mathbf{r}_s|} \right|^2 d\Omega = \int \frac{1}{|\mathbf{r}-\mathbf{r}_s|^2} d\Omega = \frac{2\pi}{rr_s} \ln \frac{r_s+r}{r_s-r} \quad (15)$$

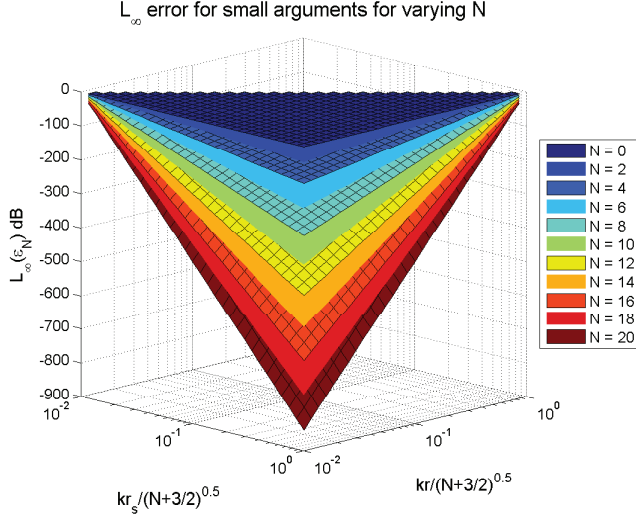


Fig. 3. L_∞ error (dB) for small kr, kr_s with N varying from 0 to 20.

Finally, we define the L_2 norm of the truncation error to signal ratio for spherical waves as

$$L_2(\epsilon_N) = \left(1 - \frac{2kr \times kr_s}{\ln[(r_s + r)/(r_s - r)]} \sum_{n=0}^N (2n+1) j_n(kr)^2 \times (j_n(kr_s)^2 + y_n(kr_s)^2) \right)^{1/2} \quad (16)$$

Figure 1 shows the plot of this error in decibels for various truncation orders against kr and kr_s . We plot the error in decibels for ease of viewing the surfaces of different orders N .

4. L_∞ ERROR

The L_∞ error represents the maximum truncation error on the sphere divided by the maximum pressure signal on the sphere due to the incoming spherical wave.

4.1. Derivation

The definition of the L_∞ error is as follows:

$$L_\infty(\epsilon_N) = \frac{\int \max |P - P_N| d\Omega}{\int \max |P| d\Omega} \quad (17)$$

We will first look at the denominator of this error, as the numerator requires certain assumptions to be made about r and r_s .

$$g_\infty = \int \max \left| \frac{e^{-ik|\mathbf{r}-\mathbf{r}_s|}}{|\mathbf{r}-\mathbf{r}_s|} \right| d\Omega \leq \int \frac{1}{r_s - r} d\Omega = \frac{4\pi}{r_s - r} \quad (18)$$

Finding the numerator of the L_∞ error requires the component functions to be replaced with their upper bounds. The spherical harmonic functions can be easily replaced using the addition theorem, eliminating a dependence on (θ, ϕ) . However the upper bounds of the spherical Bessel and Hankel functions are only valid for certain

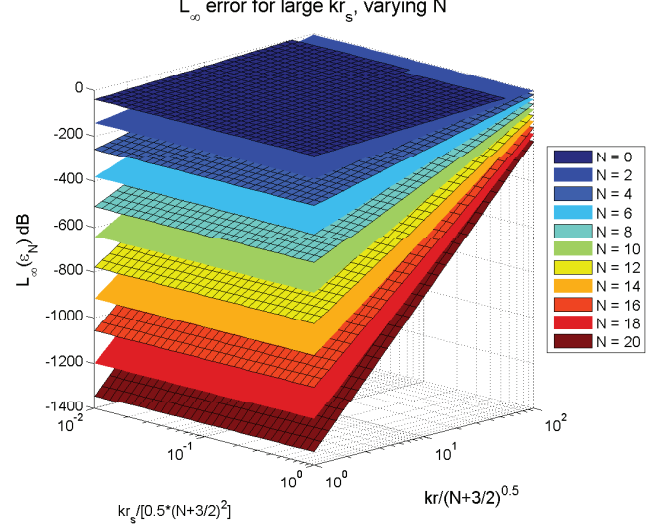


Fig. 4. L_∞ error (dB) for small kr and large kr_s with N varying from 0 to 20.

argument values. We have investigated two cases, firstly assuming that $kr, kr_s \ll \sqrt{N + \frac{3}{2}}$ and secondly that $kr \ll \sqrt{N + \frac{3}{2}}$ and $kr_s \gg (N + \frac{1}{2})^2/2$ [7]. The difference between these cases is the use of a small or large kr_s as argument to the spherical Hankel function. Figure 2 shows the small and large argument restrictions on kr_s . Note that the interior solution forces $kr < kr_s$.

The symbols z and z_s using in the following subsections refer to $kr/2$ and $kr_s/2$ respectively.

4.1.1. Small argument for the spherical Hankel function:

In this case, the small argument approximations for $j_n(kr)$ and $h_n(kr_s)$ were used. The upper bound for $|P - P_N|$ was calculated in [8] using techniques similar to [9] giving the following result for f_∞ :

$$f_\infty = 4\pi \times \left[\frac{k\pi}{2} \frac{(zz_s)^{N+1}}{\Gamma(N + \frac{3}{2})^2} \left[\frac{(N + \frac{3}{2})}{(N + \frac{3}{2})^2 - zz_s} \right] + \left(\frac{r}{r_s} \right)^{N+1} \frac{1}{r_s - r} \right] \quad (19)$$

The small argument L_∞ error is defined as (20) and it is plotted in decibels for various orders N in Figure 3 where kr and kr_s have been normalised for each N by $\sqrt{N + \frac{3}{2}}$.

$$L_\infty(\epsilon_N) = \pi(z_s - z) \frac{(zz_s)^{N+1}}{\Gamma(N + \frac{3}{2})^2} \left[\frac{(N + \frac{3}{2})}{(N + \frac{3}{2})^2 - zz_s} \right] + (z/z_s)^{N+1} \quad (20)$$

4.1.2. Large argument for the spherical Hankel function:

In this case, the small argument approximation for $j_n(kr)$ is used, while the large argument approximation for $h_n^{(2)}(kr_s)$ is used assuming $kr_s \gg (N + \frac{1}{2})^2/2$ [10].

$$h_n^{(2)}(kr_s) \leq i^{n+1} \frac{e^{-ikr_s}}{kr_s} \quad (21)$$

Using the methods described above, a result for this case is found that is quite similar to the plane wave result in [9].

$$\begin{aligned} f_\infty &= 4\pi \max \left| \sum_{n>N} j_n(kr) \sum_{m=-n}^n A_n^m Y_n^m(\theta, \phi) \right| \\ &= \frac{4\pi}{r_s} \sum_{n>N} (2n+1) |j_n(kr)| \\ &= \frac{4\pi\sqrt{\pi}}{r_s} \frac{z^{N+1}}{\Gamma(N+\frac{3}{2})} \frac{(N+\frac{3}{2})}{(N+\frac{3}{2}-z)} \end{aligned} \quad (22)$$

For small kr and large kr_s the L_∞ error is (23). This is plotted in Figure 4 for various orders N against kr and kr_s which have been normalised by $\sqrt{N+\frac{3}{2}}$ and $(N+\frac{1}{2})^2/2$ respectively. It is interesting to note that the only difference between this definition and that of the plane wave definition in [4] is a factor of $(1 - \frac{r}{r_s})$.

$$L_\infty(\epsilon_N) = \sqrt{\pi} \left(1 - \frac{z}{z_s}\right) \frac{z^{N+1}}{\Gamma(N+\frac{3}{2})} \frac{(N+\frac{3}{2})}{(N+\frac{3}{2}-z)} \quad (23)$$

5. CONVERGENCE WITH PLANE WAVES

Using the normalisation coefficient from [3] that defines a spherical wave with amplitude e^{-ikr_s}/r_s , it can be shown that the spherical harmonic coefficients of such a spherical wave converge to the equivalent plane wave as $r_s \rightarrow \infty$.

$$\begin{aligned} \lim_{r_s \rightarrow \infty} r_s e^{ikr_s} A_n^{m \text{ sph}} \\ = \lim_{r_s \rightarrow \infty} r_s e^{ikr_s} \cdot -4\pi i k h_n^{(2)}(kr_s) Y_n^{m*}(\theta_s, \phi_s) \end{aligned} \quad (24)$$

$$\begin{aligned} = \lim_{r_s \rightarrow \infty} 4\pi k r_s e^{ikr_s} i^3 i^{n+1} \frac{e^{-ikr_s}}{kr_s} Y_n^{m*}(\theta_s, \phi_s) \\ = 4\pi i^n Y_n^{m*}(\theta_s, \phi_s) = A_n^m \text{ pl} \end{aligned} \quad (25)$$

As each term of the spherical wave spherical harmonic expansion converges to the corresponding term of the plane wave, it can also be said that both the truncated signal P_N and the remainder also converge. Similarly, the L_2 spherical wave truncation error converges to the square of the plane wave result in [3].

The spherical wave L_∞ error for small arguments (Section 4.1.1) cannot converge to the plane wave result of [9] because of the assumption made about the size of kr_s . However, in the mixed argument case, where kr_s must be large, the result is very similar to that of the plane wave. If the normalisation coefficient is used and r_s is taken to ∞ , this will converge to the plane wave result.

6. DISCUSSION

The proposed norms of the truncation error show us how the spherical wave truncation error behaves with respect to wavenumber, radius, source radius and truncation order. Most importantly, as kr approaches kr_s , the error increases exponentially. Both are independent of the source direction.

These error functions are valid only for $r < r_s$ due to our use of the interior solution to the spherical wave expansion. Particularly,

the L_2 error makes no assumptions about the source wavenumber or radius, allowing it to be used in any circumstance. The L_∞ error function is useful as a simpler approximation of the maximum possible error, but has the disadvantage of only being able to be used for arguments within the limitations described in Section 4. By observation, the error decreases with kr . As such, these equations can be used to determine an appropriate truncation order, and hence number of microphones/loudspeakers required, to record or reproduce the soundfield within a particular reproduction region, or set frequency and reproduction radius limitations for a particular microphone/loudspeaker array.

The convergence of these error functions to the corresponding plane wave results is satisfying as it shows that our results are consistent with other researchers' findings.

7. CONCLUSION

In this paper we have proposed the L_2 norm and L_∞ norms for small and large arguments of the truncation error to signal ratio for spherical waves and explained their use in different circumstances. We have also shown that under certain circumstances, these error functions converge to those of the plane wave.

8. REFERENCES

- [1] B. Rafaely, "Analysis and design of spherical microphone arrays," *Speech and Audio Processing, IEEE Transactions on*, vol. 13, no. 1, pp. 135–143, 2005.
- [2] A. Laborie, R. Bruno, and S. Montoya, "A new comprehensive approach of surround sound recording," in *Audio Engineering Society Convention 114*, 3 2003. [Online]. Available: <http://www.aes.org/e-lib/browse.cfm?elib=12540>
- [3] D. B. Ward, T. D. Abhayapala, and S. Member, "Reproduction of a plane-wave sound field using an array of loudspeakers," *IEEE Trans. Speech Audio Process*, vol. 9, pp. 697–707, 2001.
- [4] T. Abhayapala, T. Pollock, and R. Kennedy, "Characterisation of 3d spatial wireless channels," vol. 1, 2003, pp. 123–127.
- [5] M. Poletti, "Unified description of ambisonics using real and complex spherical harmonics," June 2009.
- [6] E. Williams, *Fourier Acoustics: Sound Radiation and Nearfield Acoustic Holography*. London, UK: Academic Press, 1999.
- [7] M. Abramowitz and I. A. Stegun, *Handbook of Mathematical Functions with Formulas, Graphs, and Mathematical Tables*. New York: Dover Publications, 1964.
- [8] S. Brown and D. Sen, "Analysis of truncation and sampling errors in the spherical harmonic representation of soundfields." 162nd Meeting of Acoustical Society of America (accepted for publication), October 2011.
- [9] T. Abhayapala, T. Pollock, and R. Kennedy, "Characterisation of 3d spatial wireless channels," vol. 1, 2003, pp. 123–127.
- [10] L. J. Ziomek, *Fundamentals of acoustic field theory and space-time signal processing*. CRC Press, 1995.